

## ORIGINAL ARTICLE

## Effect of CYP3A perpetrators on ibrutinib exposure in healthy participants

Jan de Jong<sup>1</sup>, Donna Skee<sup>2</sup>, Joe Murphy<sup>2</sup>, Juthamas Sukbuntherng<sup>3</sup>, Peter Hellemans<sup>4</sup>, Johan Smit<sup>4</sup>, Ronald de Vries<sup>4</sup>, Juhui James Jiao<sup>2</sup>, Jan Snoeys<sup>4</sup> & Erik Mannaert<sup>4</sup>

<sup>1</sup>Janssen Research & Development, San Diego, California

<sup>2</sup>Janssen Research & Development, Raritan, New Jersey

<sup>3</sup>Pharmacyclics Inc., Sunnyvale, California

<sup>4</sup>Janssen Research & Development, Beerse, Belgium

### Keywords

Bioavailability, CYP3A perpetrators, grapefruit juice, ibrutinib, ketoconazole, rifampin

### Correspondence

Jan de Jong, 3210 Merryfield Row, San Diego, CA 92121. Tel: 1 (858) 320-3480; E-mail: jdejong1@its.jnj.com

### Funding Information

This study was supported by funding from Janssen Research & Development, LLC.

Received: 15 May 2015; Accepted: 24 May 2015

*Pharma Res Per*, 3(4), 2015, e00156, doi: 10.1002/prp2.156

doi: 10.1002/prp2.156

Previous Presentation: American Society for Clinical Pharmacology and Therapeutics (ASCP), March 18–24, 2014.

## Introduction

B-cell antigen receptor (BCR) signaling is implicated as a pivotal pathway in tumorigenesis in majority of B-cell malignancies. Antigen stimulation of normal B cells triggers dimerization of BCR initiating a downstream signaling kinase cascade, which in turn regulates multiple cellular processes, including proliferation, differentiation, apoptosis, and survival (Fuentes-Panana et al. 2004; Advani et al. 2013). Bruton's tyrosine kinase (BTK), a critical terminal kinase enzyme in the BCR signaling pathway, is a promising target for therapeutic intervention in

## Abstract

Ibrutinib (PCI-32765), a potent covalent inhibitor of Bruton's tyrosine kinase, has shown efficacy against a variety of B-cell malignancies. Given the prominent role of CYP3A in ibrutinib metabolism, effect of coadministration of CYP3A perpetrators with ibrutinib was evaluated in healthy adults. Ibrutinib (120 mg [Study 1, fasted], 560 mg [studies 2 (fasted), and 3 (nonfasted)]) was given alone and with ketoconazole [Study 1; 400 mg q.d.], rifampin [Study 2; 600 mg q.d.], and grapefruit juice [GFJ, Study 3]. Lower doses of ibrutinib were used together with CYP3A inhibitors [Study 1: 40 mg; Study 3: 140 mg], as safety precaution. Under fasted condition, ketoconazole increased ibrutinib dose-normalized (DN) exposure [DN-AUC<sub>last</sub>: 24-fold; DN-C<sub>max</sub>: 29-fold], rifampin decreased ibrutinib exposure [C<sub>max</sub>: 13-fold; AUC<sub>last</sub>: 10-fold]. Under nonfasted condition, GFJ caused a moderate increase [DN-C<sub>max</sub>: 3.5-fold; DN-AUC: 2.2-fold], most likely through inhibition of intestinal CYP3A. Half-life was not affected by CYP perpetrators indicating the interaction was mainly on first-pass extraction. All treatments were well-tolerated.

## Abbreviations

AE, adverse events; BCR, B-cell antigen receptor; BTK, Bruton's tyrosine kinase; DDI, drug–drug interaction; GFJ, grapefruit juice; LC-MS/MS, liquid chromatography–tandem mass spectroscopy; PBPK, physiologically based pharmacokinetic.

human malignancies. This downstream signal transduction protein plays a key role in the activation of pathways necessary for B-cell trafficking, chemotaxis, and adhesion, and has also been implicated in initiation, survival, and progression of mature B-cell lymphoproliferative disorders (Kuppers 2005).

Ibrutinib (Imbruvica<sup>®</sup>, PCI-32765), an orally active, BTK-targeting inhibitor, has been recently approved for the treatment of patients with chronic lymphocytic leukemia and mantle cell lymphoma who have received at least one prior therapy; Ibrutinib being the first covalent inhibitor of BTK to be advanced into human clinical trials. It

forms a stable covalent bond with cysteine-481 on the active site of BTK and irreversibly inhibits BTK phosphorylation on Tyr223, impairing BCR signaling, and disrupting the proliferation and survival of malignant B-cells ( $IC_{50}$ : 0.39 nM) (Honigberg *et al.* 2010). Ibrutinib is almost exclusively metabolized by cytochrome P450 (CYP) CYP3A. Absolute oral bioavailability ( $F$ ) is low, ranging from 3.9% in the fasted state to 8.4% following a standard breakfast without grapefruit juice (GFJ) and 15.9% with GFJ (de Vries *et al.* 2015). A major metabolite of ibrutinib, PCI-45227, is a dihydrodiol metabolite that displays reversible binding with an inhibitory activity toward BTK approximately 15 times lower than that of ibrutinib (Parmar *et al.* 2014).

Ibrutinib has a mean peak plasma concentration observed at 1–2 h after administration. The mean terminal half-life is 4–13 h, with minimum drug accumulation after repeated dosing (<twofold) (Advani *et al.* 2013; Byrd *et al.* 2013; Imbruvica™, 2014). Population pharmacokinetic (PK) analysis indicated that ibrutinib clearance is independent of age (Marostica *et al.* 2015).

Multiple medications are administered in conjunction with ibrutinib for concurrent diseases including those for opportunistic infections. Given the prominent role of CYP3A in ibrutinib metabolism, drug–drug interactions (DDIs) that affect ibrutinib exposure and its metabolites, may occur when coadministered with potent CYP3A inhibitors or inducers. It is thus essential to understand the PK profile of ibrutinib when interacting with the CYP enzyme system, which can affect drug metabolism and clearance as well as, alter their safety and efficacy profile and/or of their active metabolites.

This paper discusses results from three phase 1 studies which were undertaken to obtain a comprehensive understanding of DDI between ibrutinib and CYP3A perpetrators ketoconazole (strong inhibitor) (Study 1), rifampin (strong inducer) (Study 2), and single-strength GFJ (classified as a moderate inhibitor, specific for intestinal CYP3A) (Study 3) and their effect on ibrutinib exposure. Because it became clear during clinical development that food by itself significantly increases the relative bioavailability, Study 3 was performed in nonfasted condition. In this way, the CYP3A DDI could be assessed under more relevant conditions, and data from both fasted and nonfasted condition could be used in building a robust physiologically based pharmacokinetic (PBPK) model.

## Materials and methods

### Study population

Healthy participants (nonsmokers) aged 18–55 years (inclusive) with body mass index 18–30 kg/m<sup>2</sup> and body

weight  $\geq 50$  kg were enrolled in all three studies. Study 1 enrolled only men, whereas studies 2 and 3 enrolled both men and women.

Participants with evidence of any clinically significant medical illness that could interfere with interpretation of study results or other abnormalities in physical examination, clinical laboratory parameters, vital signs, or ECG abnormalities etc. detected at screening, were excluded from all three studies. Women were required to be postmenopausal or surgically sterile. In all three studies, participants were to refrain from taking any over-the-counter or prescribed medications except acetaminophen (<3 g per day).

Protocols for each study were approved by an Independent Ethics Committee or Institutional Review Board at each study site and the studies were conducted in accordance with the ethical principles originating in the Declaration of Helsinki and in accordance with the ICH Good Clinical Practice guidelines, applicable regulatory requirements, and in compliance with the protocol. All participants provided written informed consent to participate in the studies.

### Study design and treatment

Studies 1 and 2 were sequential design dedicated DDI studies of ibrutinib with ketoconazole and rifampin, respectively, versus Study 3, which was a two-way crossover DDI study with GFJ, combined with a formal absolute bioavailability study following single oral dose administration of ibrutinib in comparison with a single intravenous (i.v.) administration. All three studies were single center, and open-label.

Study 1 (clinicaltrials.gov identifier: NCT01626651) consisted of three phases: screening period (21 days), open-label treatment period (10 days), and follow-up period (10  $\pm$  2 days). Participants received ibrutinib (120 mg, oral) on day 1 followed by blood sampling for PK analysis upto 72 h. Ketoconazole (Tara Pharmaceuticals), 400 mg oral, was given once-daily (q.d.) from days 4 to 9 (except on day 7); on day 7 they received ibrutinib (40 mg, oral) in combination with ketoconazole (400 mg, oral) 1 h before ibrutinib dosing.

Study 2 (clinicaltrials.gov identifier: NCT01763021) consisted of screening period (21 days), open-label treatment period (14 days) and follow-up period (10  $\pm$  2 days). Participants received ibrutinib, 560 mg, oral, q.d. on day 1. Rifampin (VersaPharm) 600 mg oral, q.d. was given from days 4 to 13 (after the last ibrutinib sample collection for PK [over 72 h]). On day 11, a second single oral dose of ibrutinib 560 mg was administered, followed by the blood sample collection over 72 h.

In studies 1 and 2, ibrutinib was administered after overnight fast; food was withheld for 4 h after ibrutinib administration on dosing days.

Study 3 (clinicaltrials.gov identifier: NCT01866033) consisted of screening period (21 days), open-label treatment period (treatment A, B and C) (19 days), and follow-up period ( $10 \pm 2$  days). All participants received ibrutinib (560 mg) in treatment A and then randomized to either treatment B (ibrutinib [560 mg] administered 30 min after 240 mL of glucose in water) or treatment C (240 mL of GFJ [Albert Heijn pink] the evening before and 30 min before ibrutinib [140 mg]). In treatments B and C, participants had standard breakfast 30 min after ibrutinib dosing, as opposed to treatment A which was given in fasted condition. A single i.v. dose of 100  $\mu\text{g}$   $^{13}\text{C}_6$  PCI-32765 was administered 2 h after each ibrutinib oral dose.

In all three studies, participants took ibrutinib with 240 mL of water and lunch and subsequent standard meals were provided 4 h after oral ibrutinib dosing. Participants remained seated throughout morning (from 30 min before dosing until after lunch), in order to minimize inter and intrasubject intestinal blood flow differences.

## Pharmacokinetic evaluations

### Sample collection

Blood samples for all studies were collected by direct venipuncture or through an indwelling peripheral venous heparin lock catheter into heparin collection tubes. Samples were centrifuged at approximately 4°C (15 min at 1300 g); plasma was stored at  $\leq -70^\circ\text{C}$ .

Blood samples for PK analysis were collected predose and 0.5, 1, 1.5, 2, 3, 4, 6, 8, 12, 16, 24, 48, and 72 h post-dose on days 1 and 7 (Study 1 and 3) and days 1 and 11 (Study 2) for quantification of ibrutinib and PCI-45227. Additional blood samples were collected 2 h after ketoconazole dosing on day 7 (1 h after ibrutinib dosing) (Study 1) and 2 h after rifampin dosing on day 11 (Study 2) for ketoconazole and rifampin measurement, respectively. In Study 2, samples were collected and analyzed for determination of 4- $\beta$ -hydroxycholesterol concentration on day -1, 12 h after ibrutinib administration on day 11 and 14.

### Analytical methods

Plasma concentrations of ibrutinib, its metabolite, PCI-45227, ketoconazole, rifampin, and  $^{13}\text{C}_6$  ibrutinib, were determined using validated analytical liquid chromatography-tandem mass spectroscopy (LC-MS/MS) methods. Bioanalyses were conducted at Department of Bioanalysis, Janssen R&D and at Frontage Laboratories, Inc., Exton, PA.

Quantification range was 0.100–25.0 ng/mL for ibrutinib and PCI-45227 (Study 1 and 2) and 0.5–100 ng/mL (Study 3) (de Vries et al. 2015). Quantification range for  $^{13}\text{C}_6$  PCI-32765 was 2–1000 pg/mL (de Vries et al. 2015).

### Pharmacokinetic analysis

PK analyses were performed by noncompartmental methods using validated WinNonlin® software Version 5.2.1 (Certara USA, Inc. Princeton, NJ) and Phoenix WinNonlin 6.3. Key PK parameters included maximum observed plasma concentration ( $C_{\text{max}}$ ), time to reach maximum observed plasma concentration ( $t_{\text{max}}$ ), elimination half-life associated with terminal slope ( $\lambda_z$ ) of the semilogarithmic drug concentration-time curve ( $t_{1/2\lambda}$ ), area under the plasma concentration-time curve (AUC) from time 0 to 24 h ( $\text{AUC}_{24}$ ), AUC from time 0 to time of the last quantifiable concentration ( $\text{AUC}_{\text{last}}$ ), AUC from time 0 to infinity ( $\text{AUC}_{\infty}$ ) and metabolite/parent ratios. In Study 1, apparent total clearance of drug after extravascular administration ( $\text{CL}/F$ ), and apparent volume of distribution based on the terminal phase ( $\text{Vd}_z$ ) were also estimated. Additionally, in Study 3, absolute bioavailability ( $F$ ) and total clearance of drug after i.v. administration ( $\text{CL}$ ) were also estimated.

### Safety evaluations

Safety evaluations included assessments of treatment-related adverse events (AE), vital signs, 12-lead electrocardiograms, clinical laboratory tests, and physical examinations. The AE severity was graded according to the National Cancer Institute - Common Terminology Criteria for Adverse Events (NCI-CTCAE) grading system version 4.03.

### Analysis sets

Participants who had estimations of PK parameters of ibrutinib for both periods (ibrutinib administered alone and in combination with CYP3A perpetrators) were included in PK analysis set for statistical comparison. Participants who received at least one dose of study medication were included in safety analysis set.

### Sample size determination

For all three studies, sample size determinations were based on statistical estimation. A sample size is considered adequate if the point estimates of GMR for PK parameters of primary interest ( $C_{\text{max}}$ , AUCs) fall within the no-effect boundaries of clinical equivalence (90% CI) to the compound.

## Statistical analyses

All individual and mean plasma concentrations and estimated PK parameters were presented by graphic and descriptive statistics methods for each treatment. Linear mixed-effect models were applied to evaluate potential DDI effect. Log-transformation was performed on PK parameters ( $C_{\max}$ , AUCs) prior to the analysis, and 90% confidence intervals for GMR (with/without coadministration of interacting drugs) were constructed on original scale.

## Results

### Subject disposition and demographics

All enrolled participants (Study 1:  $n = 18$ ; Study 3:  $n = 8$ ) completed studies 1 and 3. In Study 2, 17/18 enrolled participants completed the study. One participant was excluded from the PK-evaluable population due to a protocol deviation (use of prohibited concomitant pain medication). Demographics and baseline characteristics of the participants in three studies were consistent with the inclusion and exclusion criteria (Table 1). All participants received scheduled doses of the study drugs.

### Pharmacokinetic results

#### Study 1: effect of ketoconazole on pharmacokinetics of ibrutinib and its metabolite

Following coadministration of ibrutinib with ketoconazole under fasted condition, mean DN\_ $C_{\max}$  (dose normalized to 120 mg) of ibrutinib increased from 11.8 to 325 ng/mL and mean DN\_ $AUC_{\text{last}}$  increased from 71.4 to 1599 ng-h/mL (Fig. 1A). Although dose proportionality was not formally tested for ibrutinib, no deviations from linearity were observed neither in the Phase I escalating dose study nor population PK study (imbruvica™ 2014; Marostica et al. 2015), thus justifying the dose-normalization of ibrutinib exposure in this study. Intersubject variability in ibrutinib+ketoconazole treated participants for both  $C_{\max}$  and  $AUC_{\text{last}}$  were >50% following ibrutinib administration alone and approximately 40% when coadministered with ketoconazole. The  $V_d/F$  and  $CL/F$  were both lower following ibrutinib + ketoconazole compared with ibrutinib alone ( $V_d/F$ : 885 L vs. 19049 L;  $CL/F$ : 92.0 L/h vs. 2014 L/h, whereas there was no change in mean  $t_{\max}$  (2.00 h vs. 1.75 h) and  $t_{1/2}$  (6.32 h vs. 8.20 h) (Table S1).

On the other hand, dose-normalized PCI-45227 exposure was lower following coadministration with ketoconazole compared with ibrutinib administration alone (Fig. 1B). The DN\_ $C_{\max}$  was 2.6 times lower (11.1 ng/mL

**Table 1.** Demographics and baseline characteristics (safety analysis set).

	Study 1 <sup>1</sup> ( $n = 18$ )	Study 2 <sup>2</sup> ( $n = 18$ )	Study 3 <sup>3</sup> ( $n = 8$ )
Sex, $n$			
Women	–	8	5
Men	18	10	3
Race, $n$ (%)			
White	4 (22)	5 (28)	8 (100)
Black or African American	11 (61)	11 (61)	–
Other/multiple	2 (11)	2 (11)	–
Ethnicity, $n$ (%)			
Not Hispanic or Latino	16 (89)	16 (89)	8 (100)
Hispanic or Latino	2 (11)	2 (11)	0
Age (years)			
Mean (SD)	33.7 (8.8)	41.1 (11.6)	46.4 (8.1)
Baseline weight (kg)			
Mean (SD)	78.0 (7.4)	77.6 (8.7)	70.0 (13.2)
Baseline BMI (kg/m <sup>2</sup> )			
Mean (SD)	26.1 (2.3)	26.4 (2.5)	23.5 (2.7)

BMI, body mass index; GFJ, grapefruit juice; SD, standard deviation.

<sup>1</sup>Study 1: ibrutinib + ketoconazole.

<sup>2</sup>Study 2: ibrutinib + rifampin.

<sup>3</sup>Study 3: ibrutinib + grapefruit juice.

vs. 29.1 ng/mL) and DN\_ $AUC_{\text{last}}$  was 1.2 times lower (256 ng-h/mL vs. 304 ng h/mL) following ibrutinib + ketoconazole treatment compared with ibrutinib alone. Intersubject variability for both  $C_{\max}$  and  $AUC_{\text{last}}$  was approximately 40% following ibrutinib administration alone and approximately 20% following ibrutinib + ketoconazole.  $T_{\max}$  and  $t_{1/2}$  were both slightly longer following ibrutinib + ketoconazole ( $T_{\max}$ : 4.00 h vs. 2.00 h;  $t_{1/2}$  18.00 h vs. 11.41 h). Following coadministration with ketoconazole, ibrutinib mean DN\_ $C_{\max}$  increased approximately 29-fold (geometric mean [GM]: 285.49 vs. 10.0 ng/mL), and mean DN\_ $AUC_{\text{last}}$  increased approximately 24-fold (GM: 1463.43 vs. 61.16 ng-h/mL) (Table 2). Mean metabolite to parent ratios decreased from 2.64 to 0.05 for  $C_{\max}$  and from 5.03 to 0.19 for  $AUC_{24}$  following ibrutinib+ketoconazole coadministration.

Plasma concentrations for ketoconazole at 1 h after drug intake on day 7 ranged from 231 to 15,800 ng/mL. Two participants had very low ketoconazole concentrations (352 ng/mL and 231 ng/mL); the interaction was still within the observed range.

#### Study 2: effect of rifampin on the pharmacokinetics of ibrutinib and its metabolite

Following coadministration with rifampin under fasted condition, ibrutinib mean  $C_{\max}$  and  $AUC_{\text{last}}$  decreased ( $C_{\max}$ : 42.1 ng/mL to 3.38 ng/mL;  $AUC_{\text{last}}$ : 335 ng-h/mL

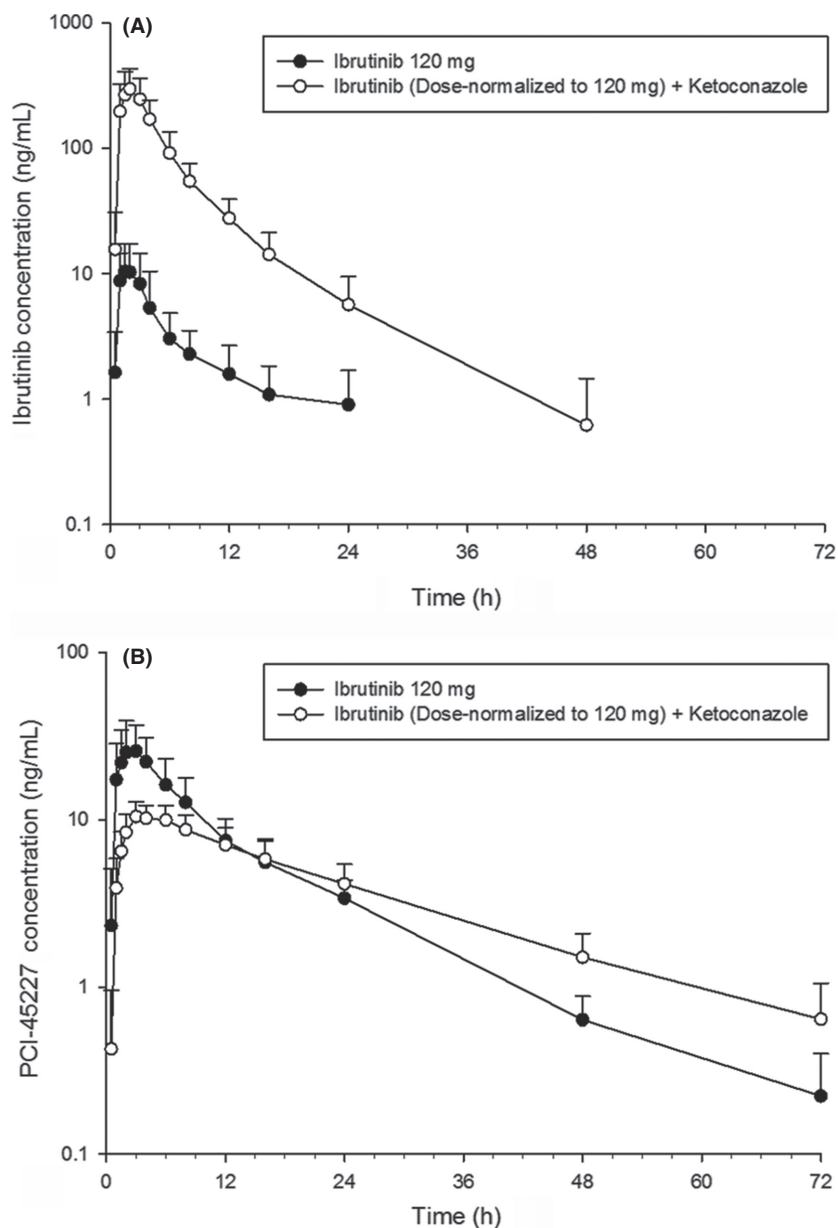


**Figure 1.** Dose-normalized mean (SD) logarithmic-linear plasma concentration-time profiles following oral administration of ibrutinib (120 mg) alone (day 1) and in combination with ketoconazole (40 mg Ibrutinib+400 mg Ketoconazole) (day 7) to healthy men. (A) Ibrutinib; (B) PCI-45227.

to 38.0 ng·h/mL) compared with ibrutinib administration alone (Fig. 2A). Intersubject variability for both  $C_{max}$  and  $AUC_{last}$  was greater than 60% following ibrutinib administration alone and greater than 70% following ibrutinib+rifampin. Median  $t_{max}$  was delayed from 1.76 to 3.00 h. Terminal  $t_{1/2}$  was similar; due to multiple data points below the quantification limit in the elimination phase, it could only be calculated for 5 of 17 participants.

Following coadministration with rifampin, PCI-45227 mean  $C_{max}$  decreased from 70.0 ng/mL to 49.9 ng/mL and mean  $AUC_{last}$  decreased from 946 ng·h/mL to

374 ng·h/mL (Fig. 2B). Intersubject variability for both  $C_{max}$  and  $AUC_{last}$  was greater than 30% following ibrutinib administration alone and greater than 20% following ibrutinib + rifampin. Similar to the parent, median  $t_{max}$  of the metabolite was delayed following ibrutinib + rifampin coadministration compared with ibrutinib treatment alone (from 2.02 to 3.00 h). Terminal  $t_{1/2}$  trended shorter for the combination treatment. The GMR for  $C_{max}$  and  $AUC_{last}$  was 7.94% and 10.44% (or a 13- and 10-fold decrease), respectively, for ibrutinib + rifampin compared with ibrutinib alone (Table 2). Metabolite to parent ratio

# Explore Litigation Insights

Docket Alarm provides insights to develop a more informed litigation strategy and the peace of mind of knowing you're on top of things.

## Real-Time Litigation Alerts



Keep your litigation team up-to-date with **real-time alerts** and advanced team management tools built for the enterprise, all while greatly reducing PACER spend.

Our comprehensive service means we can handle Federal, State, and Administrative courts across the country.

## Advanced Docket Research



With over 230 million records, Docket Alarm's cloud-native docket research platform finds what other services can't. Coverage includes Federal, State, plus PTAB, TTAB, ITC and NLRB decisions, all in one place.

Identify arguments that have been successful in the past with full text, pinpoint searching. Link to case law cited within any court document via Fastcase.

## Analytics At Your Fingertips



Learn what happened the last time a particular judge, opposing counsel or company faced cases similar to yours.

Advanced out-of-the-box PTAB and TTAB analytics are always at your fingertips.

## API

Docket Alarm offers a powerful API (application programming interface) to developers that want to integrate case filings into their apps.

## LAW FIRMS

Build custom dashboards for your attorneys and clients with live data direct from the court.

Automate many repetitive legal tasks like conflict checks, document management, and marketing.

## FINANCIAL INSTITUTIONS

Litigation and bankruptcy checks for companies and debtors.

## E-DISCOVERY AND LEGAL VENDORS

Sync your system to PACER to automate legal marketing.